ACS APPLIED MATERIALS & INTERFACES

www.acsami.org

Research Article

Functional Ginger-Derived Extracellular Vesicles-Coated ZIF-8 Containing TNF-α siRNA for Ulcerative Colitis Therapy by Modulating Gut Microbiota

Chenyang Cui, Miao Du, Yihang Zhao, Jiaze Tang, Mengge Liu, Geng Min, Rongchen Chen, Qiang Zhang, Zhaowei Sun,* and Haibo Weng*

Cite This: https://doi.org/10.1021/acsami.4c10562

Read Online

ACCESS | Metrics & More | Article Recommendations | Supporting Information

ABSTRACT: Tumor necrosis factor-α (TNF-α) plays a causal role in the pathogenesis of ulcerative colitis (UC), and anti-TNF-α siRNA shows great promise in UC therapy. However, delivering siRNA with site-targeted stability and therapeutic efficacy is still challenging due to the complex and dynamic intestinal microenvironment. Here, based on the functional plant-derived ginger extracellular vesicles (EVs) and porous ZIF-8 nanoparticles, we propose a novel TNF-α siRNA delivery strategy (EVs@ZIF-8@siRNA) for UC targeted therapy. Ginger EVs show strong colon and macrophage targeting, as well as robust resistance to acidic degradation in the stomach. Moreover, 6-shogaol in ginger-derived EVs displays anti-inflammatory effects, which enhance the treatment efficiency by cooperation with TNF-α siRNA. *In vitro* experiments reveal that ZIF-8 nanoparticles have high TNF-α siRNA loading capacity and promote siRNA escape from cellular lysosomes. *In vivo* experiments show that the TNF-α level is reduced more significantly in colonic tissue than other nontargeted inflammation related factors, showing a good targeting of this composite nanoparticle. Furthermore, gut microbiota sequencing results demonstrate that the nanoparticles can promote intestinal barrier repair by regulating the intestinal microbial balance and restoring the intestinal health of UC mice. Therefore, the developed EVs@ZIF-8@siRNA nanoparticles may represent a novel colon-targeted oral drug, providing a promising therapeutic strategy for UC therapy.

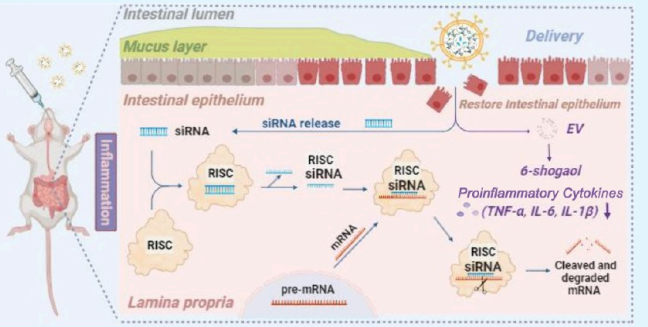

KEYWORDS: *Ulcerative colitis, TNF-α, Ginger EVs, siRNA delivery, ZIF-8*

1. INTRODUCTION

Ulcerative colitis (UC) is an intractable and long-term chronic inflammatory bowel disease with prevalence and incidence continuously increasing.[1,2] The incidence of cases is estimated to be 5 million worldwide in 2023.[3,4] Typical symptoms of UC patients include abdominal pain, diarrhea, emaciation, and bloody stools,[5,6] which are closely related to the defect of the intestinal epithelial barrier, dysregulation of microbiota, and adverse immune response.[7] Although many therapeutic agents such as 5-amino salicylic acid, steroid hormones, and some inhibitors have been provided over the past decades, most UC patients still struggle with long-term burdensome complications or debilitating side effects because of their high doses usage and nonspecific effects on the immune system.[8] TNF-α as a crucial pro-inflammatory cytokine has been proven to disrupt cellar membrane integrity and promote intestinal inflammation.[9−11] So, suppressing excessive TNF-α has become an effective therapeutic strategy for UC, such as use of TNF-α monoclonal antibody.[12] However, the method of systemic administration is toxic and ineffective, limiting clinical application.[13,14] Therefore, a new therapeutic approach with high specificity and low systemic toxicity is considerably critical for UC treatment.

A small interfering RNA (siRNA)-based therapeutic is safe and efficient, and growing evidence indicates that remission has been achieved in UC patients after treatment with anti-TNF-α siRNA.[15−20] However, naked siRNA is unable to cross the cell membrane because of its hydrophilic and anionic properties, and it is sensitive to nuclease and cannot effectively silence the TNF-α gene in tissues.[21−23] Therefore, many siRNA carriers have been proposed. Cell-derived extracellular vesicles (EVs) have attracted wide attention due to their natural nanoscale size, good biocompatibility, and stability in

Received: June 25, 2024
Revised: September 10, 2024
Accepted: September 11, 2024
Published: September 20, 2024

Scheme 1. EVs@ZIF-8@siRNA Nano-delivery System for the Treatment of UC. (A) Preparation Process of EVs@ZIF-8@siRNA. (B) EVs@ZIF-8@siRNA Specifically Treated UC

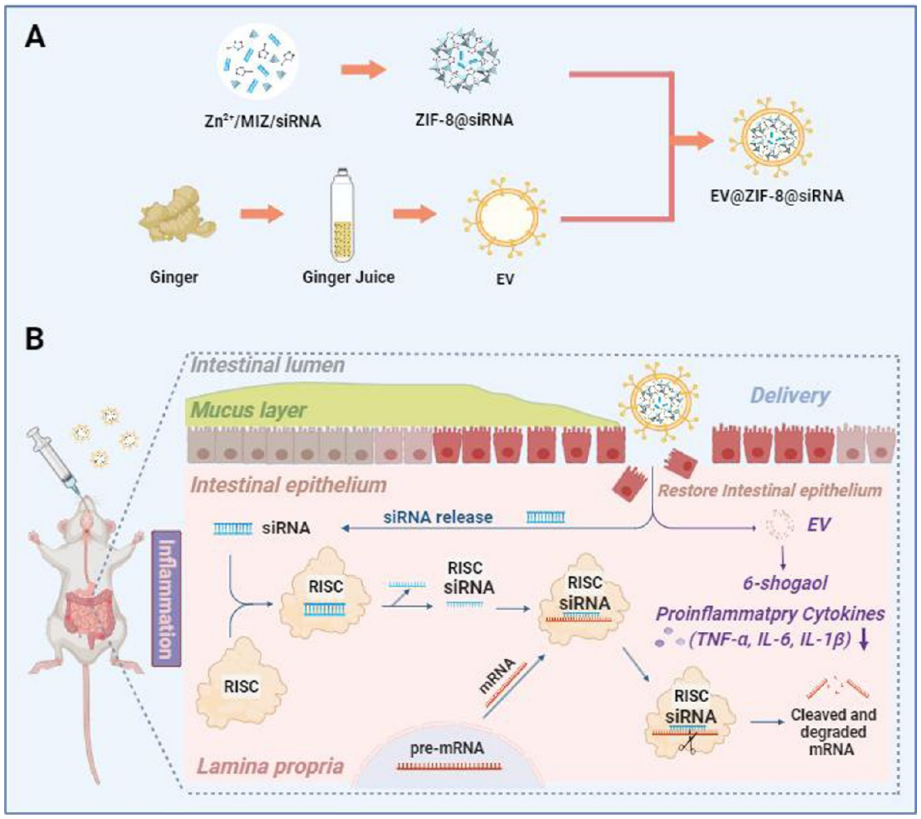

the circulatory system.[24,25] However, limitations still exist for EVs in clinical practice. First, loading approaches such as electroporation, sonication, and passive incubation are unstable and inefficient.[26] Second, the proteins on EVs are complex and vary depending on the parent-cells, which need to be addressed or modified to avoid off-target toxicity to normal tissues.[27] Last but not least, cell-derived EVs are not facilely harvested but require several days to culture large-scale cells, making it difficult to meet the requirements for clinical application.

Ginger is a traditional Chinese food and medicine, in which the active substance, 6-shogaol, possesses antioxidant, anti-inflammatory, and anticancer effects.[28−30] Recently, Zhang's group demonstrated that ginger-derived EVs could avoid the hydrolysis of digestive enzymes in the stomach and are preferentially distributed in the intestine tissues after oral administration.[31] These findings indicate that ginger-derived EVs are suitable as siRNA delivery carriers for UC treatment. However, loading sufficient siRNA into ginger EVs can be challenging. Therefore, a novel siRNA delivery system is proposed in this work using ginger-derived EVs-coated ZIF-8 to overcome the above-mentioned problems. As shown in Scheme 1, several goals can be achieved: (1) ZIF-8 has the advantages of porosity, large specific surface area, and room temperature synthesis, which enable it to load siRNA efficiently and easily;[32−34] (2) ginger EVs have good colon tissue targeting, ensuring the loaded siRNA silences the expression of TNF-α specifically without off-target toxicity; (3) ginger EVs contain 6-shogaol, which can reduce the levels of inflammatory factors (TNF-α, IL-6, and IL-1β) and work synergistically with siRNA to repair intestinal inflammation;[35,36] (4) ginger is edible, low-cost, and readily available in bulk, making it possible to obtain mass amounts of EVs quickly and easily to accelerate results in clinical settings. To the best of our knowledge, ginger-derived EVs-coated ZIF-8 nanoparticles for UC siRNA therapy have not been described, which may provide a new avenue for studying the siRNA delivery system through plant-derived EVs combined with nanoparticles for UC treatment.

2. EXPERIMENTAL SECTION

2.1. Chemicals and Reagents. 2-Methylimidazole and zinc nitrate hexahydrate were ordered from Sigma-Aldrich (MO, USA). The MTT Cell Proliferation and Cytotoxicity Assay Kit was purchased from EnoGene (Nanjing, China). Dextran sulfate sodium (DSS, colitis grade, MW = 36−50 kDa) was ordered from MP Biomedicals (CA, USA). The RNA extraction kit and reverse transcription kit were purchased from Beibei Biotechnology Co. Ltd. (Zhengzhou, China). The PCR kit was ordered from Synomebio Co., Ltd. (Shanghai, China). The StarLighter HP SYBR Green qPCR Mix was purchased from Foreverstar Biotech (Beijng, China). RNase and RNase free water were ordered from Novoprotein (Shanghai, China). TNF-α siRNA (sense: 5′- GUCUCAGCCUCUUCU-CAUUCCUGCT-3′, antisense: 5′- AGCAGGAAUGAGAAGAGG-CUGAGACAU-3′), carboxyl fluorescein (FAM)-labeled siRNA, TNF-α, IL-6 and IL-1β primers were synthesized from Tsingke Biotechnology Co., Ltd. (Beijing, China). Cy5.5-labeled-siRNA was synthesized from Bioligo Biotechnology (Shanghai) Co., Ltd. (Shanghai, China). The BCA protein concentration detection kit, RPMI 1640 culture-medium and 4% polyformaldehyde were purchased from Solarbio Science & Technology Co., Ltd. (Beijing, China). Uranium deoxy acetate and 200 mesh copper mesh were purchased from Zhongjingkeyi Technology Co., Ltd. (Beijing, China). FBS was ordered from Gibco (CA, USA). DAPI and LysoTracker were provided by Beyotime (Shanghai, China). ELISA kits for TNF-α (SEKM-0034) and IL-1β (SEKM-0002) cytokines were purchased

https://doi.org/10.1021/acsami.4c10562
ACS Appl. Mater. Interfaces XXXX, XXX, XXX−XXX

from Solarbio Science & Technology Co., Ltd. (Beijing, China). ELISA kits for IL-6 (JL20268) were ordered from Jianglai biology (Shanghai, China). The myeloperoxidase (MPO) test kit was purchased from Nanjing Jiancheng Bioengineering Institute (Nanjing, China). 6-Shogaol standard product was purchased from Shanghai Chen Microbial Technology Co., Ltd. (Shanghai, China).

2.2. Preparation of ZIF-8 Nanoparticles. ZIF-8 nanoparticles were synthesized according to the previously reported method with slight modification.[37] First, 2-methylimidazole and siRNA with different concentrations were mixed in an aqueous solution at pH 8, and then zinc nitrate hexahydrate was added dropwise. After vortex stirring for 30 s, the mixture solution was allowed to stand for 4 h and centrifuged with PBS (pH 8) to remove excess siRNA. Then, ZIF-8 nanoparticles containing siRNA (ZIF-8@siRNA) were collected after drying overnight under reduced pressure at 60 °C. The final concentrations of zinc nitrate hexahydrate and 2-methylimidazole were 1 and 20 mg/mL, respectively. The input concentration of siRNA ranged from 50 to 200 nmol. Unless otherwise specified, 200 nmol of siRNA was used to synthesize ZIF-8@siRNA nanoparticles. FAM and Cy5.5-labeled siRNAs (FAM siRNA and Cy5.5-siRNA) were prepared for further use.

2.3. Extraction and Purification of EVs. Ginger-derived EVs were extracted and purified based on a reported method.[35,38] Fresh ginger was bought from a local market and washed with deionized water. The ginger juice was collected and differentially centrifuged at 3000*g* for 20 min, 10000*g* for 40 min, and 150,000*g* for 2 h to isolate exosome-like nanoparticles. Then, the sediment was resuspended in PBS before centrifugation at 150,000*g* for 2 h on a sucrose gradient (8%, 15%, 30%, 45% and 60%) to obtain the purified ginger EVs. A BCA protein concentration detection kit was used to determine the total protein concentration on the EVs membrane. The amount of EVs was 100 ng obtained from 1 kg of ginger.

2.4. Preparation of EVs@ZIF-8@siRNA Nanoparticles. To obtained EVs coated ZIF-8@siRNA nanoparticles, ZIF-8@siRNA (1 mg/mL) was mixed with EVs (0.5 mg/mL). After fusing for 30 min by ultrasonication, the mixture was continuously extruded through polycarbonate porous membranes (Millipore, Germany) with pore sizes of 800, 400, 200, and 100 nm, respectively, using a liposome extruder (Morgec Machinery, Shanghai, China). Subsequently, EVs@ZIF-8@siRNA nanoparticles were collected after centrifugation at 12000 rpm for 5 min and resuspended in PBS solution at 4 °C for further use.

2.5. Characterization of Nanoparticles. The size and surface zeta potential of EVs, ZIF-8, ZIF-8@siRNA and EVs@ZIF-8@siRNA nanoparticles were measured by a Malvern particle size analyzer (Mastersizer 2000, UK). The morphology of the nanoparticles was observed by transmission electron microscopy (TEM) (Hitachi, Japan). For sample preparation, 10 μL of fully mixed nanoparticles was dropped into a 200 mesh copper mesh (Zhongjingkeyi Technology Co., Ltd., Beijing, China). After incubation for 30 s, 10 μL of 2% uranoxy acetate was dropped for another 60 s (only for EVs and EVs@ZIF-8@siRNA). EVs@ZIF-8@siRNA nanoparticles were also subjected to an element mapping analysis. The crystallographic information of ZIF-8 and ZIF-8@siRNA nanoparticles was analyzed by powder X-ray diffraction (Bruker, Germany). The specific surface area information of ZIF-8 and ZIF-8@siRNA nanoparticles was collected by a fully automated specific surface area analyzer (Micromeritics, GA, USA). To quantify the encapsulation efficiency of siRNA in ZIF-8, we used different concentrations of FAM-siRNA to prepare the ZIF-8@FAM-siRNA nanoparticles. After collection, the nanoparticles were resuspended and collapsed in an aqueous solution at pH 3 to release FAM-siRNA. Then, the fluorescence intensity of the supernatant (F_1) was measured using a BioTek Synergy Mx microplate reader (excitation/emission = 494/520 nm). The fluorescence intensity of the initial FAM-siRNA solution was detected and recorded as F_0. The calculation formula for encapsulation efficiency (F%) is $F\% = F_1/F_0 \times 100\%$.

2.6. Cell Cultures. Mouse RAW264.7 cells, human Caco-2 cells and human HT-29 cells (provided by the Cell Bank of Chinese Academy of Sciences) were cultured in RPMI 1640 and DMEM medium containing 10% fetal bovine serum (FBS) and cultured in a 75 cm^2 flasks at 37 °C in a humidified atmosphere containing 5% (v/v) CO_2. The medium was changed every 2 to 3 days. After the cells were fully grown, the cells were collected in a cryopreservation tube (SAINING Biotechnology) and cryopreserved in liquid nitrogen.

2.7. Cell Internalization. RAW264.7 cells were inoculated into the laser confocal dish (NEST Biotechnology, Wuxi, China) with 4×10^4 cells per well. ZIF-8@FAM-siRNA and EVs@ZIF-8@FAM-siRNA were added per well and incubated with cells for 3, 8, and 12 h, respectively. The quantities of ZIF-8@FAM-siRNA and EVs@ZIF-8@FAM-siRNA were 5 μg, and the input amount of FAM-siRNA was 0.5 nmol. Then, the medium was discarded, and cells were washed with PBS three times. Immediately, fresh media containing LysoTracker was added to stain the lysosomes for 30 min at 37 °C. After being washed with PBS three times, the cells were fixed with 4% paraformaldehyde for 20 min and subsequently stained with DAPI at 37 °C for 30 min. Samples were observed by laser scanning confocal microscopy with a 63 X oil-mirror lens (Leica, Germany). ImageJ software was used to analyze the average fluorescence intensity of the images.

2.8. Flow Cytometry. RAW264.7 cells were inoculated into a 6-well plate (KIRGEN) with 4×10^4 cells per well. ZIF-8@FAM-siRNA and EVs@ZIF-8@FAM-siRNA with 0.5 nmol of input concentration of FAM-siRNA were added and incubated with cells for 12 h. After being cleaned with PBS three times, cells were digested with trypsin for 5 min, and then digestion was stopped with fresh medium. The cells precipitates were collected and resuspended with 200 μL of PBS after centrifugation at 1500 rpm for 5 min and detected by a FongCyte flow cytometer (Challenbio, Beijing, China). Flow cytometry data were analyzed by using FloJo-V10.

2.9. Cell Viability Assay. The cell viability was detected by MTT assay.[39] RAW264.7 cells, Caco-2 cells, and human HT-29 cells were inoculated into 96-well plates (PakGent Bioscience (Suzhou) Co., Ltd.) with 3×10^3 cells per well, and this was repeated 5 times. After cultivation overnight, siRNA, ZIF-8, EVs, EVs@ZIF-8, ZIF-8@siRNA and EVs@ZIF-8@siRNA were added and incubated with cells for 12, 24 and 48 h, respectively. The quantities of EVs, EVs@ZIF-8, and EVs@ZIF-8@siRNA were 5 μg, and the input amount of siRNA was 0.5 nmol. Each well was incubated with 20 μL MTT for 4 h, and the cell viability was measured by a multimode reader at 490 nm.

2.10. RT-PCR/qRT-PCR. Total RNA in colon tissue was extracted and reverse-transcribed into cDNA using a reverse transcription kit. Then, the mRNA levels of TNF-α, IL-6 and IL-1β were analyzed using a fluorescent quantitative PCR kit. The primer sequences of qPCR are as follows: TNF-α, 5′-AGGCTGCCCCGACTACGT-3′ (forward) and 5′-GACTTTCTCCTGGTA TGAGATAGCAAA-3′ (reverse); IL-6, 5′-ACAAGTCGGAGGCTTAATTACACA T-3′ (forward) and 5′-TTGCCATCCGCACAACTCTTTTC-3′ (reverse); IL-1β, 5′-TCGCTCAGGGTCACAAGAAA-3′ (forward) and 5′-CATCAG AGGCAAGGAGGAAAAC-3′ (reverse).

2.11. Induction and Treatment of UC. All animal experiments were approved by the Ethics Committee of Zhengzhou University. C57BL/6 female mice were purchased from Charles River (Beijing, China). After several days of adaptation, 6 week old mice were given 3% DSS orally for 7 consecutive days to establish UC model and fed with water as control.[40] UC mice were randomly divided into 6 groups (siRNA, ZIF-8, EVs, EVs@ZIF-8, ZIF-8@siRNA and EVs@ZIF-8@siRNA) with 5 mice each and administrated daily with nanoparticles containing 200 nmol of siRNA for 5 consecutive days to study the therapeutic effect. During the period of UC induction, the drinking water was changed on days 1, 3 and 5, and the rat cage was changed daily. The weight of mice was recorded and the stool state was observed. After 5 days of oral administration, the mice were euthanized, and the colon tissue was collected for the length measurement and H&E staining.

2.12. *In Vivo* Targeting Experiment. Cy5.5-labeled siRNA (Cy5.5-siRNA) was used to investigate the targeting of nanoparticles *in vivo*. Free Cy5.5-siRNA, ZIF-8@Cy5.5-siRNA and EVs@ZIF-8@Cy5.5-siRNA with a dose of 200 nmol of siRNA were injected into C57BL/6 mice, respectively. After oral administration for 24 h, the

https://doi.org/10.1021/acsami.4c10562
ACS Appl. Mater. Interfaces XXXX, XXX, XXX−XXX

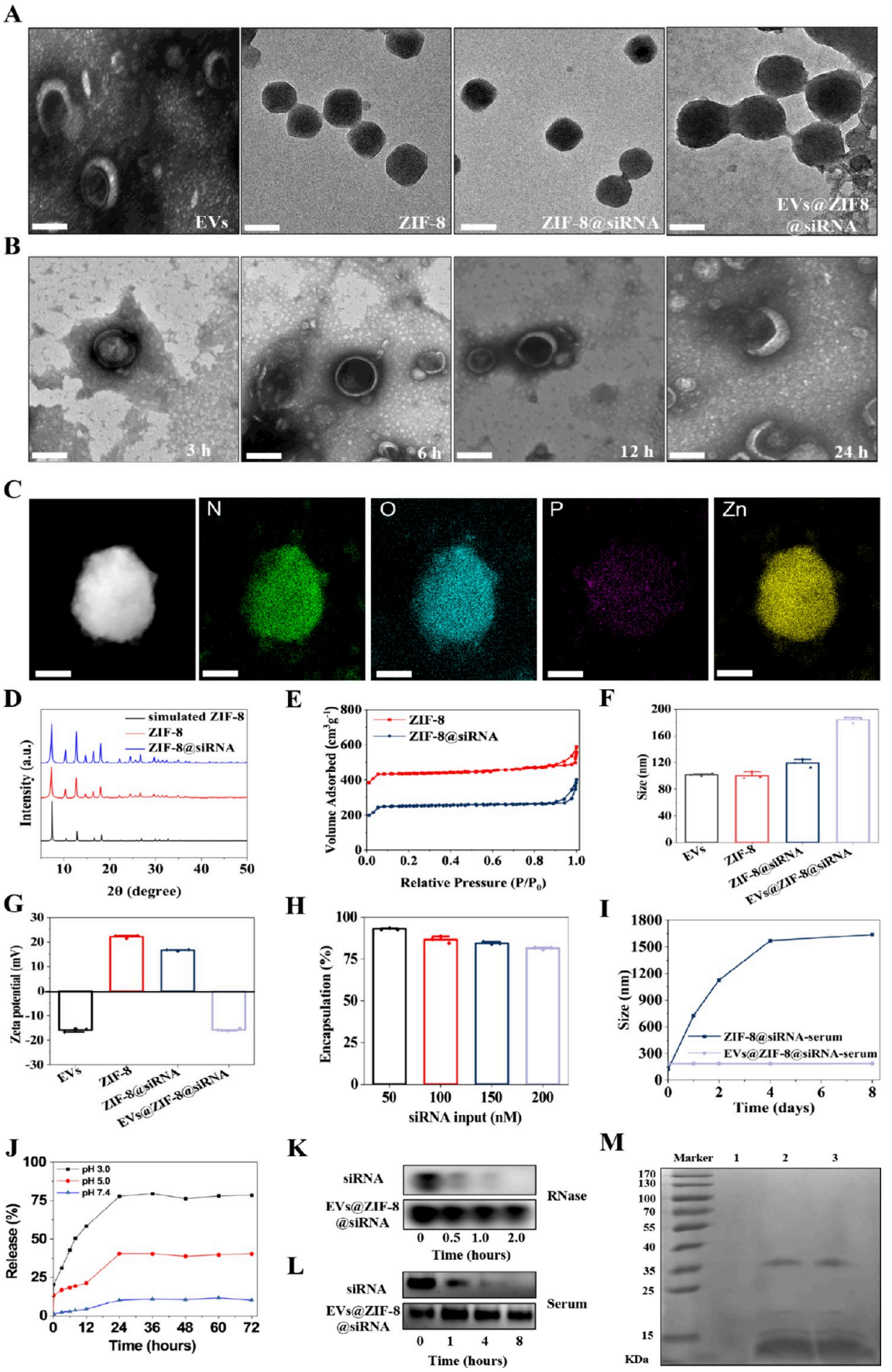

Figure 1. Characterization of EVs@ZIF-8@siRNA. (A) TEM images of EVs, ZIF-8, ZIF-8@siRNA and EVs@ZIF-8@siRNA (scale bar = 100 nm). (B) TEM images of EVs after being dissolved in PBS at pH 3.0 for 3, 6, 12, and 24 h (scale bar = 100 nm). (C) TEM elemental mapping images of

https://doi.org/10.1021/acsami.4c10562
ACS Appl. Mater. Interfaces XXXX, XXX, XXX−XXX

Figure 1. continued

EVs@ZIF-8@siRNA. (D) XRD patterns of ZIF-8 and ZIF-8@siRNA. (E) N_2 adsorption−desorption isotherms of ZIF-8 and ZIF-8@siRNA. (F) Diameter sizes of EVs, ZIF-8, ZIF-8@siRNA and EVs@ZIF-8@siRNA (n = 3). (G) Zeta potentials of EVs, ZIF-8, ZIF-8@siRNA and EVs@ZIF-8@siRNA (n = 3). (H) Encapsulation efficiency of siRNA in EVs@ZIF-8@siRNA with different concentrations (n = 3). (I) Stability of ZIF-8@siRNA and EVs@ZIF-8@siRNA in serum over time (n = 3). (J) Release rates of siRNA from EVs@ZIF-8@siRNA in PBS at different pH values over time (n = 3). (K) Agarose gel electrophoresis results of bare siRNA and EVs@ZIF-8@siRNA after incubating with RNase and (L) serum-containing medium. (M) SDS-PAGE protein analysis of ZIF-8, EVs and EVs@ZIF-8@siRNA (1: ZIF-8, 2: EVs, 3: EVs@ZIF-8@siRNA).

mice were anesthetized with a small animal anesthetic (Changsha Meyue Biotechnology Co., Ltd., Hunan, China) and euthanized. The main organs of colon, heart, lung, liver, spleen, and kidney of mice were collected and observed by an IVIS spectroscopic small animal optical imaging system (PerkinElmer, MA, USA).

2.13. Enzyme-Linked Immunosorbent Assay (ELISA). The ELISA detection method was based as described in literature reports with slight modification.[41,42] In order to detect cytokines, RAW264.7 cells were inoculated into six-well plates with 4×10^4 cells and incubated for 24 h. Then, the medium was replaced with fresh containing LPS (150 ng/mL) for stimulation. After 12 h, siRNA, ZIF-8, EVs, EVs@ZIF-8, ZIF-8@siRNA and EVs@ZIF-8@siRNA with 0.5 nmol input concentration of siRNA were added and incubated with cells for 24 h. The cell supernatant was collected, and the contents of TNF-α, IL-6 and IL-1β were detected by an ELISA kit. The colon tissue was homogenized and centrifuged at 12000 rpm for 15 min to remove insoluble substances, and the content of TNF-α, IL-6, and IL-1β in the supernatant was measured.

2.14. Determination of Myeloperoxidase (MPO). MPO was determined according to previously reported methods and was shown to be slightly improved.[35] 0.5 g of colon tissue was taken up and cleaned with cold PBS for 3 times. Supernatant was obtained and determined with a myeloperoxidase kit.

2.15. *In Vivo* Safety Test. To investigate the safety of nanoparticles, normal female C57BL/6 mice were divided into two groups with 3 mice and injected with EVs@ZIF-8@siRNA nanoparticles and PBS, respectively. After 24 h, the major organs and the tissue sections of the mice were collected and H&E and fluorescent TUNEL staining were performed.

2.16. 16S rRNA Sequencing and Microbiome Analysis. Fresh feces from each group of mice (n = 6) were collected, and DNA was extracted for 16S rRNA sequencing analysis (Shanghai Personal Biotechnology Co., Ltd.). Briefly, PCR amplification of the 16S rRNA gene was performed using 338F (5′-ACTCCTACGGGAGGCAGCA-3′) and 806R (5′-GGACTACHVGGGTWTCTAAT-3′) primers, followed by library construction and sequencing. β-Diversity was analyzed with principal coordinates analysis (PCoA). Linear discriminant analysis effect size (LEfSe) was performed for phyla and genera. Cladogram was analyzed for the taxonomic tree of differentially abundant taxa. An unweighted UniFrac distance matrix was used for the UPGMA clustering analysis, and the clustering results were integrated with the relative species abundance of each sample at the phylum and genus levels.

2.17. Statistical Analysis. The data were expressed as the mean ± standard deviation with three independent tests. Statistical analysis was conducted via GraphPad Prism 8.0, Origin 2021 and R Studio (4.1.3) software. The significant difference was verified by t-test and marked by asterisk ($^*P < 0.05$, $^{**}P < 0.01$, and $^{***}P < 0.001$, respectively). All compounds are >95% pure by analysis. HPLC trace data are given in the Supporting Information (Table S1).

3. RESULTS AND DISCUSSION

3.1. Characterization of EVs@ZIF-8@siRNA. The EVs@ZIF-8@siRNA nanoparticle was prepared, as illustrated in Scheme 1. ZIF-8@siRNA was first prepared by *in situ* synthesis and then coated with ginger-derived EVs to construct a core−shell like structure. The preparation process of this system was simple, convenient and fast. However, it must be carried out strictly under no RNA enzyme aqueous solution at pH 8.0 to prevent the degradation of siRNA before encapsulation in ZIF-8. Transmission electron microscopy (TEM) images displayed that ginger-derived EVs exhibited a typical spherical shape, ZIF-8 and ZIF-8@siRNA showed a uniform octahedral shape, and EVs@ZIF-8@siRNA exhibited a smooth surface and typical core−shell structure, suggesting that EVs-coated ZIF-8@siRNA nanoparticles were successfully synthesized (Figure 1A). The stability in acidic solution of ginger EVs was also verified. As shown in Figure 1B and Figure S1, EVs exhibited complete spherical shapes and uniform size after dissolving in acidic solution for 3, 6 and 12 h but began to rupture and increase in size after 24 h (Figure 1B and Figure S1). The results indicated that ginger EVs could remain intact in an acidic environment at least for 12 h, which is enough time for them to cross the stomach and reach colon tissue. The acid resistance of ginger EVs may be attributed to the following points: first, the combination of lipids and proteins, as well as the glycoproteins and polysaccharides on the EVs membrane surface possesses a protective barrier; second, acid−base buffering substances within EVs regulate internal pH levels to maintain a stable environment.[36,43] Moreover, TEM element mapping images showed that N, O, P, and Zn elements were homogeneously distributed on the EVs@ZIF-8@siRNA surface, in which the N element indicated that siRNA was loaded and the P element represented the existence of EVs. The results suggested that the composite nanoparticles were successfully synthesized (Figure 1C). The powder X-ray diffraction (PXRD) was also measured and revealed that ZIF-8 displayed good crystallinity with the typical diffraction peaks corresponding to the simulated, and no obvious shifts were observed after loading with siRNA, which indicated that loading siRNA did not affect the crystalline structure of ZIF-8 (Figure 1D). Nitrogen adsorption−desorption isotherm experiments were also conducted. As depicted in Figure 1E, ZIF-8 and ZIF-8@siRNA exhibited the typical I-shape, suggesting they possessed microporous structures capable of carrying large amounts of siRNA. Compared with ZIF-8, the BET surface area and micropore volume of ZIF-8@siRNA were significantly reduced because of the occupation of miRNA in the cavity, indicating the successful payload of siRNA. The size and potential of nanoparticles were also characterized. As shown in Figure 1F and G, the size of the EV was 80.36 nm with a −15.92 mV potential, while a 183.85 nm size was obtained in EVs@ZIF-8@siRNA, suggesting that a composite nanoparticle was acquired. Meanwhile, the size of ZIF-8 increased from 96.87 to 118.71 nm after loading the siRNA, and the potential decreased from 22.24 mV to 16.68 mV and further decreased to −15.83 mV after coating with EVs. These results indicated that EVs@ZIF-8@siRNA nanoparticles were successfully synthesized. Next, the loading amount of siRNA was determined by using FAM-labeled siRNA. Figure 1H shows that ZIF-8 could load siRNA efficiently over a wide range of inputs attributed to its large nanopore size as well as the strong electrostatic interaction

https://doi.org/10.1021/acsami.4c10562
ACS Appl. Mater. Interfaces XXXX, XXX, XXX−XXX

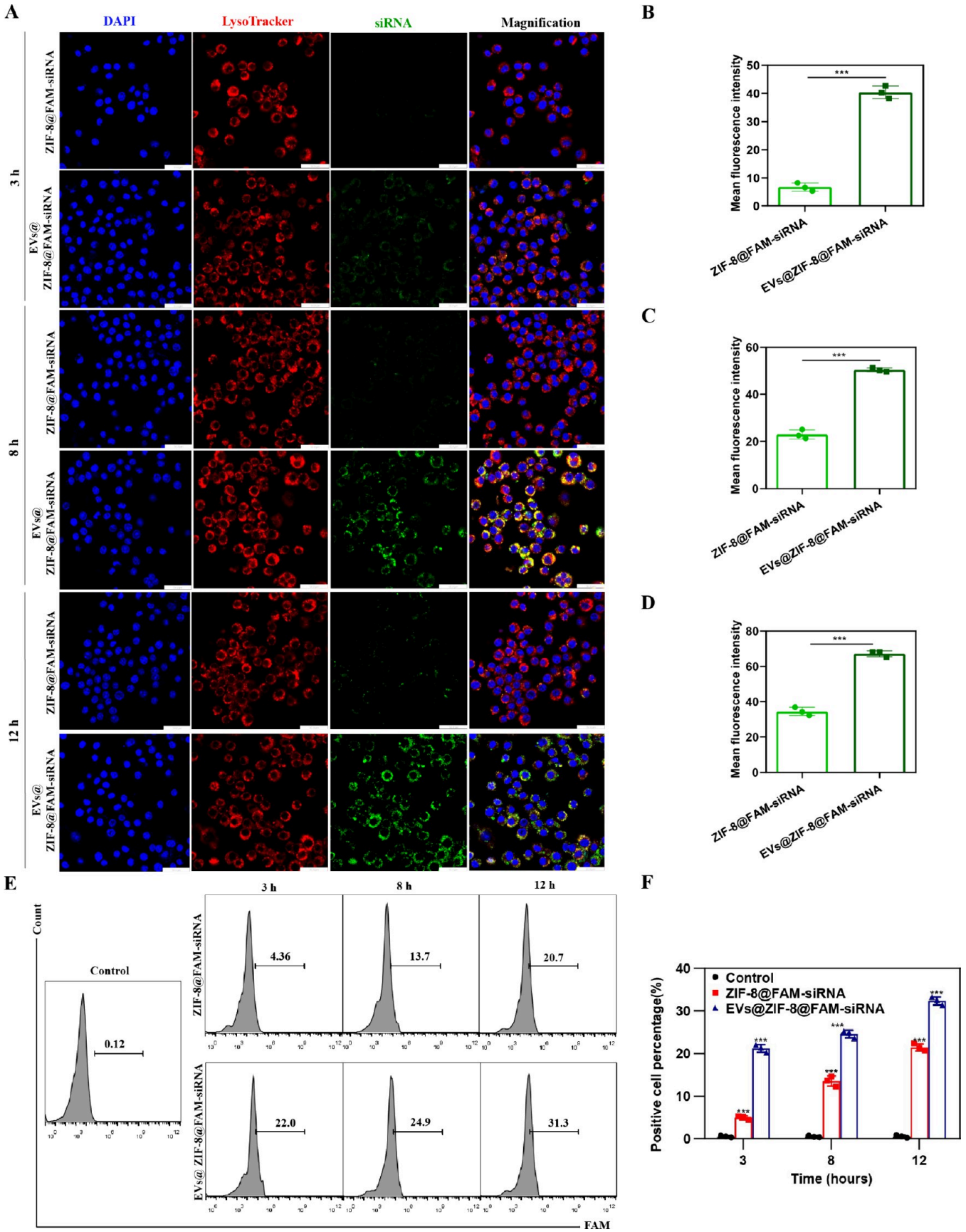

Figure 2. Cellular internalization of ZIF-8@siRNA and EVs@ZIF-8@siRNA. (A–D) Laser confocal images and green fluorescence quantitative analysis of RAW 264.7 cells after incubation with ZIF-8@siRNA and EVs@ZIF-8@siRNA for 3, 8 and 12 h (scale = 36.8 μm; nucleus, blue; lysosome, red; siRNA, green; $n = 3$). (E–F) Fluorescence quantitative analysis of RAW 264.7 cells by flow cytometry ($n = 3$). Data are presented as the means ± SD. *** $P < 0.001$.

https://doi.org/10.1021/acsami.4c10562
ACS Appl. Mater. Interfaces XXXX, XXX, XXX–XXX

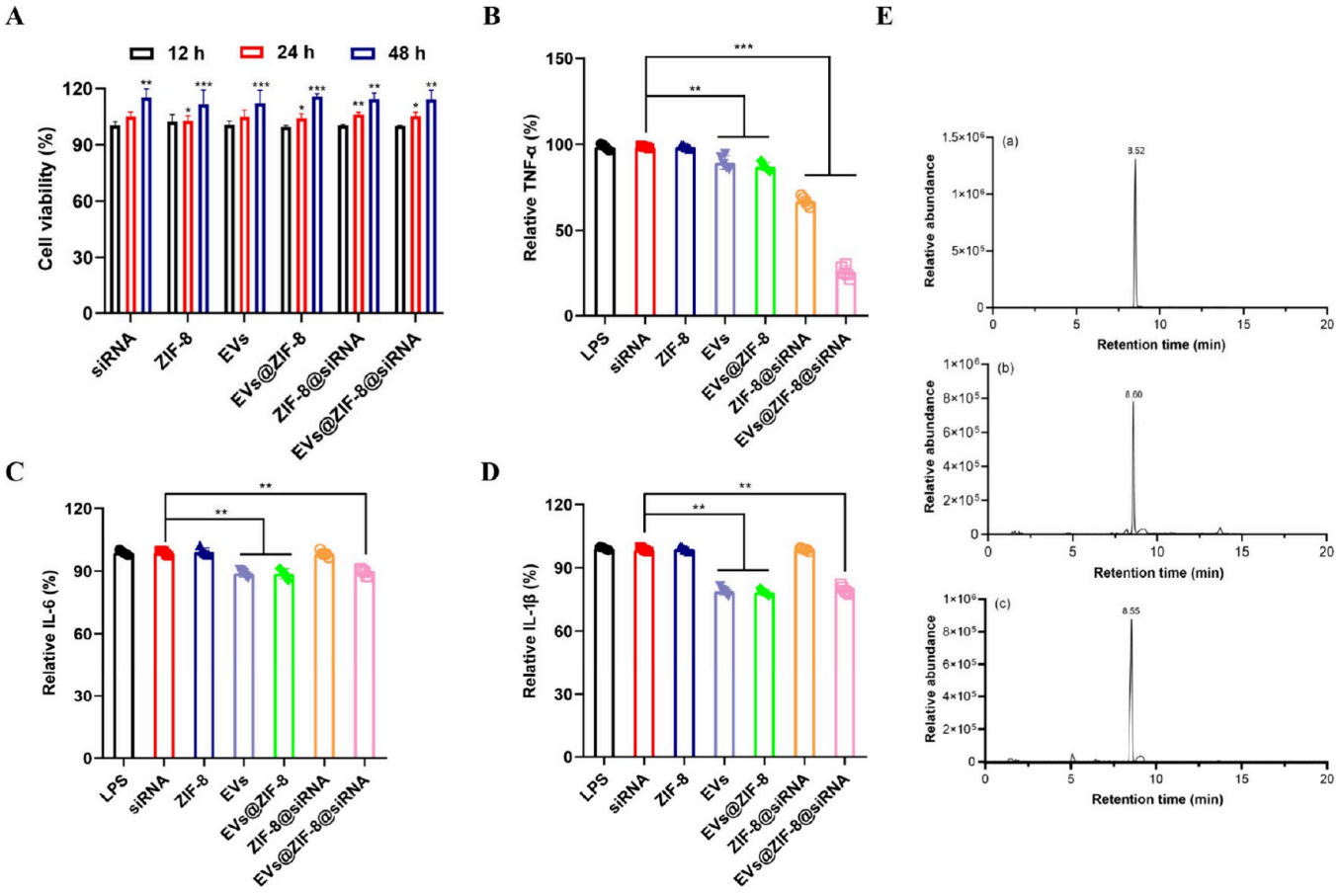

Figure 3. Effect of EVs@ZIF-8@siRNA on RAW 264.7 cells *in vitro*. (A) The effects of different nanoparticles on the viability of RAW 264.7 cells. (B) The contents of TNF-α, (C) IL-6 and (D) IL-1β in RAW 264.7 cells treated with different nanoparticles were determined by ELISA (n = 3). (E) HPLC of 6-shogaol in different nanoparticles (a: standards; b: EVs; c: EVs@ZIF-8@siRNA). Data are presented as the means ± SD. *P < 0.05, **P < 0.01, ***P < 0.001.

between the metal nodes in ZIF and the backbone phosphates of siRNA.[44] In the subsequent experiments, EVs@ZIF-8@siRNA nanoparticles were prepared using 200 nM siRNA, 20 mg/mL 2-methylimidazole and 1 mg/mL zinc nitrate hexahydrate.

The biocompatibility of EVs@ZIF-8@siRNA nanoparticles was evaluated by incubating them with serum medium. The size of EVs@ZIF-8@siRNA nanoparticles exhibited minimal change compared with ZIF-8@siRNA nanoparticles, which rapidly increased to 1.5 μm, indicating EVs showed important roles in ZIF stability and biocompatibility under physiological conditions (Figure 1I).[45,46] The stability of the EVs@ZIF-8@siRNA nanocarriers was measured in PBS at different pH values. Under pH 7.4 conditions, the size of the EVs@ZIF-8@siRNA nanocarriers showed minimal change. However, at pH 3.0 and pH 5.0, the size of the EVs@ZIF-8@siRNA nanocarriers was first decreased and then increased to around 500 nm (Figure S3). In the first 12 h, the size of the EVs@ZIF-8@siRNA nanocarriers decreased slightly, which benefits from the protective effect of EVs. However, a continuing decrease in size to 50 nm was observed at pH 3.0, suggesting the structure of EVs@ZIF-8@siRNA nanoparticles was degraded. The subsequent size increase may be due to the aggregation of the components in EVs@ZIF-8@siRNA nanoparticles with the acidic medium components in buffer to form new complexes.[47] In addition, siRNA release rates in EVs@ZIF-8@siRNA nanoparticles were measured in PBS at different pH values. As shown in Figure 1J, the amount of siRNA released gradually increased with the extension of time, peaked at 24 h, and then tended to stabilize. Compared with pH 5.0 and pH 7.4, the release rate of siRNA was highest at pH 3.0, with 75%, which may be due to the rupture of EVs in acidic environment observed in Figure 1B.[48] The protective effect of EVs@ZIF-8 nanoparticles on the siRNA integrity was also investigated. Results of agarose gel electrophoresis (AGE) showed that free siRNA can be degraded by RNase and serum in a short time, while little degradation was observed in EVs@ZIF-8@siRNA, which confirmed that EVs@ZIF-8 nanoparticles had a good protective efficacy on the stability of siRNA (Figure 1K and L). Furthermore, the expressions of EVs-derived proteins on EVs@ZIF-8@siRNA nanoparticles were also verified by SDS-PAGE (Figure 1M), demonstrating that ginger EVs were successfully coated on the surface of ZIF-8@siRNA nanoparticles. After being stored at −80 °C for 48 h, the reproducibility of ginger EVs was evaluated by SDS-PAGE, DLS and TEM, and results showed that EVs had good reproducibility in terms of composition, nanometer size and morphology (Figure S4).

3.2. Cellular Internalization of EVs@ZIF-8@siRNA. The intracellular transport and uptake efficiency of EVs@ZIF-8@siRNA nanoparticles were investigated by incubating with RAW264.7 cells (Figure 2A–D and Figure S1). After co-incubation with 3 h, a small amount of siRNA (green) was observed in the EVs@ZIF-8@FAM-siRNA group, while

https://doi.org/10.1021/acsami.4c10562
ACS Appl. Mater. Interfaces XXXX, XXX, XXX−XXX

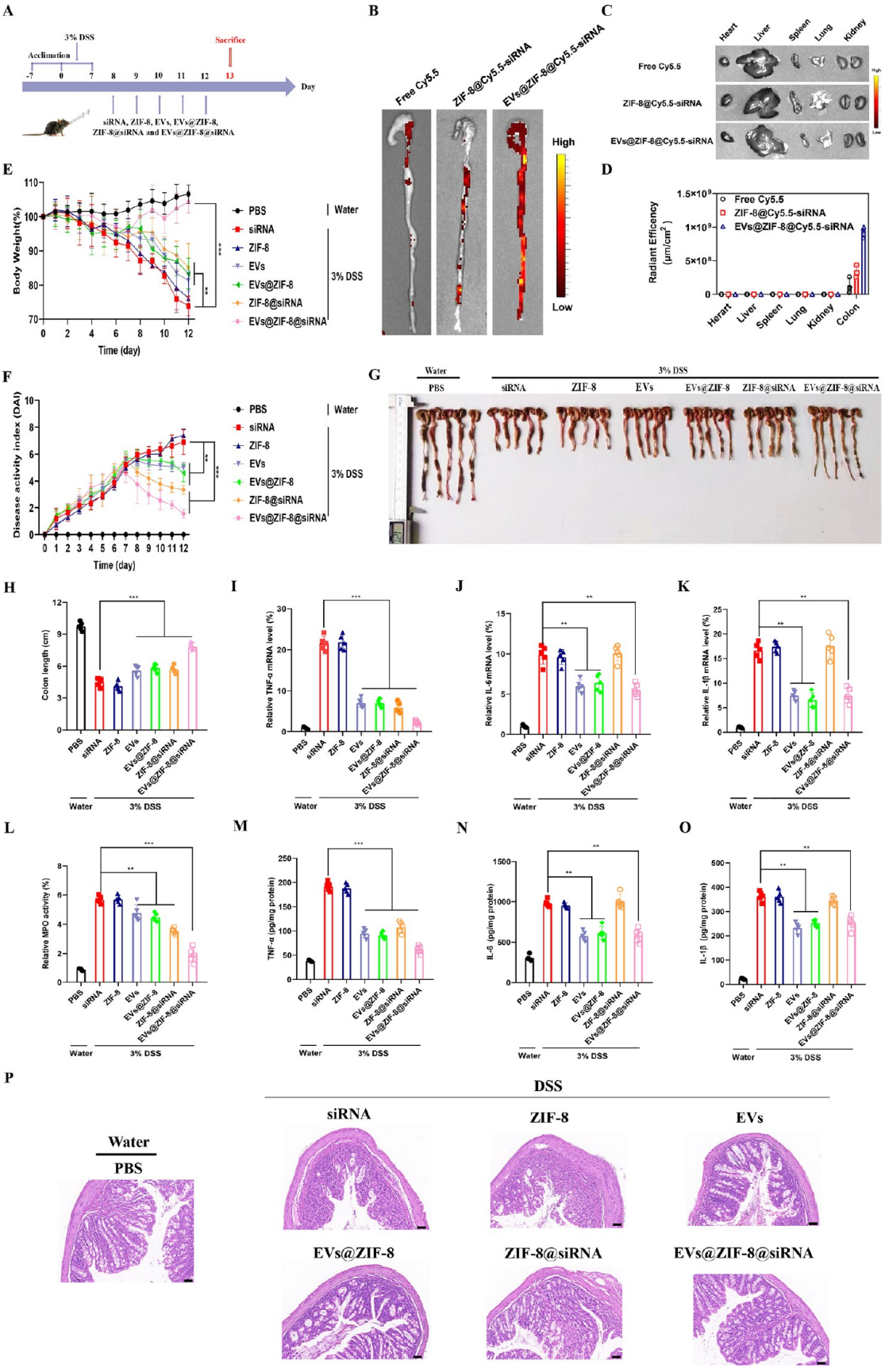

Figure 4. Therapeutic effect of EVs@ZIF-8@siRNA *in vivo*. (A) Schematic diagram of induction and treatment of a mouse UC model. C57BL/6 mice were fed 3% DSS for 7 days to induce the UC model and then treated with siRNA, ZIF-8, EVs, EVs@ZIF-8, ZIF-8@siRNA, and EVs@ZIF-8@siRNA for 5 consecutive days. The daily dose of siRNA for each mouse was 200 nmol. The mice were euthanized on the sixth day, and colon tissues were collected for analysis. (B−C) Fluorescence distributions of colon tissue and major organs after treatment with free Cy5.5, ZIF-8@

https://doi.org/10.1021/acsami.4c10562
ACS Appl. Mater. Interfaces XXXX, XXX, XXX−XXX

Figure 4. continued

Cy5.5-siRNA and EVs@ZIF-8@Cy5.5-siRNA for 24 h (n = 3). (D) Quantitative analysis of fluorescence intensity in spleen, kidney, liver and colon tissue (n = 3). (E) Body weight, (F) index of disease activity (DAI), (G) colon tissue images, and (H) colon length of mice after treatment with different nanoparticles (n = 5). (I−K) Quantitative RT-PCR of TNF-α, IL-6 and IL-1β mRNA in colon (n = 5). (L) Relative MPO activity in colon tissue. (M−O) Expression levels of TNF-α, IL-6 and IL-1β in colon tissues by ELISA (n = 5). (P) Representative H&E staining images of colon tissue (scale bar = 50 μm). Data are presented as the means ± SD. $^{**}P < 0.01$, $^{***}P < 0.001$.

negligible green fluorescence was observed in the ZIF-8@FAM-siRNA. These results indicated that ginger EVs encapsulation increases the uptake rate of nanoparticles by cells due to their improved biocompatibility, enhanced permeability and retention effect (EPR effect).[49−51] After 8 h of co-incubation, the green fluorescence intensity in the EVs@ZIF-8@FAM-siRNA group was more obvious, and it was even more pronounced after 12 h incubation. Meanwhile, a colocalization of siRNA with lysosomes (red) was observed in the EVs@ZIF-8@FAM-siRNA group, which indicated that large amounts of siRNA in nanoparticles entered the lysosome. After being incubated with cells for 12 h, the red fluorescence was reduced in the EVs@ZIF-8@FAM-siRNA group, while green fluorescence was distributed in various parts of the cytoplasm, which suggested that siRNA escaped effectively from the lysosome and entered the cytoplasm as acid sensitive ZIF-8 nanoparticles. Then, the fluorescence intensity of FAM-siRNA in RAW264.7 cells was quantitatively analyzed by flow cytometry (Figure 2E, F). The results showed that the fluorescence intensity of the EVs@ZIF-8@siRNA group was higher than that of the bare ZIF-8@siRNA group, which was consistent with the results observed by confocal laser microscopy. Zhang's group demonstrated the high affinity of ginger-derived EVs for macrophages, which was consistent with our results that ZIF-8 coated with ginger EVs can effectively improve cell targeting and siRNA uptake efficiency.[35]

3.3. Inhibition of EVs@ZIF-8@siRNA *In Vitro*. The safety of nanoparticles on RAW264.7 cells, Caco-2 cells, and HT-29 cells was first explored, and the results showed that different nanoparticles did not affect the cell activity compared with free siRNA (Figure 3A, S4 and S5), indicating that nanoparticles have good safety in cells. Next, the concentration of TNF-α in RAW 264.7 cells was measured, and it is shown in Figure 3B. There were no differences between the control group (LPS) and siRNA group, while a significant reduction was observed in the groups of ZIF-8@siRNA and EVs@ZIF-8@siRNA, indicating that free siRNA hardly enters cells owing to its negative charge and easy degradation properties, but delivery vectors significantly enhanced the cell internalization of siRNA. EVs alone and EVs@ZIF-8 groups also showed reductions in the TNF-α expressions, indicating that the EVs derived from ginger exhibited anti-inflammatory effects.[12] High performance liquid chromatography (HPLC) results further confirmed that ginger-derived EVs contain 6-shogaol, an active ingredient capable of reducing the levels of inflammatory factors, and the content of 6-shogaol in EVs and EVs@ZIF-8@siRNA was 2.56 μg/mg and 2.52 μg/mg, respectively (Figure 3E and Table S1).[36] So, the group of EVs@ZIF-8@siRNA reduced TNF-α levels the most, with 74%, which benefited from the enhanced siRNA uptake as well as the anti-inflammatory effect of ginger EVs.

To further investigate the anti-inflammatory effects of EVs@ZIF-8@siRNA nanoparticles, we have also detected non-targeted pro-inflammatory factors concentrations. As the main inflammatory immune cells, macrophages played an important role in the occurrence and development of inflammation and secreted a variety of pro-inflammatory factors when stimulated by inflammation.[41,52,53] So, the concentrations of IL-6 and IL-1β in RAW 264.7 cells were also measured. From Figure 3C, D, we found that groups of EV alone, EVs@ZIF-8, and EVs@ZIF-8@siRNA showed abilities in reducing IL-6 and IL-1β levels (Figure 3C, D), which demonstrated that ginger-derived EVs have anti-inflammatory effects and can combine with TNF-α siRNA to enhance the treatment of UC.

3.4. Treatment of EVs@ZIF-8@siRNA *In Vivo*. Ginger-derived EVs have been reported to be more likely absorbed by gut bacteria in the colon due to their abundant phosphatidic acid (PA), so the targeting of EVs@ZIF-8@siRNA was explored by using the UC mouse model (Figure 4A).[43] Colonic fluorescence imaging on mice was performed after oral administration of Cy5.5-labeled EVs for 24 h. Results showed that ginger EVs coating nanoparticles were more concentrated in colon tissue, 6 times higher than the ZIF-8@siRNA treated group, while only a small amount of fluorescence was observed in the Cy5.5 group (Figure 4B, D). In addition, the fluorescence signals of other major organs (heart, liver, spleen, lung, and kidney) were negligible throughout the examined period, indicating that EVs@ZIF-8@siRNA was metabolized in the GI tract after oral administration (Figure 4C, D). These results demonstrated that ginger-derived EVs modification on the ZIF-8@siRNA nanoparticles surface greatly enhanced the colon tissue targeting and can efficiently deliver siRNA to the colon tissue *in vivo*.[54,55]

Weight loss and shortened colon length were typical pathological features of DSS induced mice, so their parameters were recorded during the whole period.[56] As shown in Figure 4E, compared with the naked siRNA, mice treated with EVs@ZIF-8@siRNA had significantly increased body weight, close to that of normal controls, indicating a good growing status of mice after treatment with EVs@ZIF-8@siRNA. Meanwhile, both ZIF-8@siRNA and EVs@ZIF-8 partly increased body weight compared to the free siRNA or ZIF-8 groups because of the vital role of vectors in siRNA therapy and the anti-inflammatory effects of ginger EVs (Figure 4E). To evaluate the therapeutic effects of nanoparticles, the disease activity index (DAI), a composite score that reflects the severity of the disease, was measured.[57] Figure 4F displays that the composite score for control mice was 0, while DSS mice treated with siRNA had a high score, suggesting a serious disease was pronounced in DSS mice because free siRNA had difficulty entering cells and hardly affected the target TNF-α in colon tissue. After treatment with EVs, EVs@ZIF-8 or ZIF-8@siRNA, the DAI score was reduced, which further demonstrated that ginger EVs were capable of anti-inflammatory effects and ZIF-8 can deliver siRNA effectively. Consistent with *in vitro* results, DSS mice treated with the EVs@ZIF-8@siRNA group exhibited a notable lowest score, demonstrating that mice had an obvious remission owing to the cooperation effects of ginger EVs and siRNA (Figure 4F). Next, the colon

https://doi.org/10.1021/acsami.4c10562
ACS Appl. Mater. Interfaces XXXX, XXX, XXX−XXX

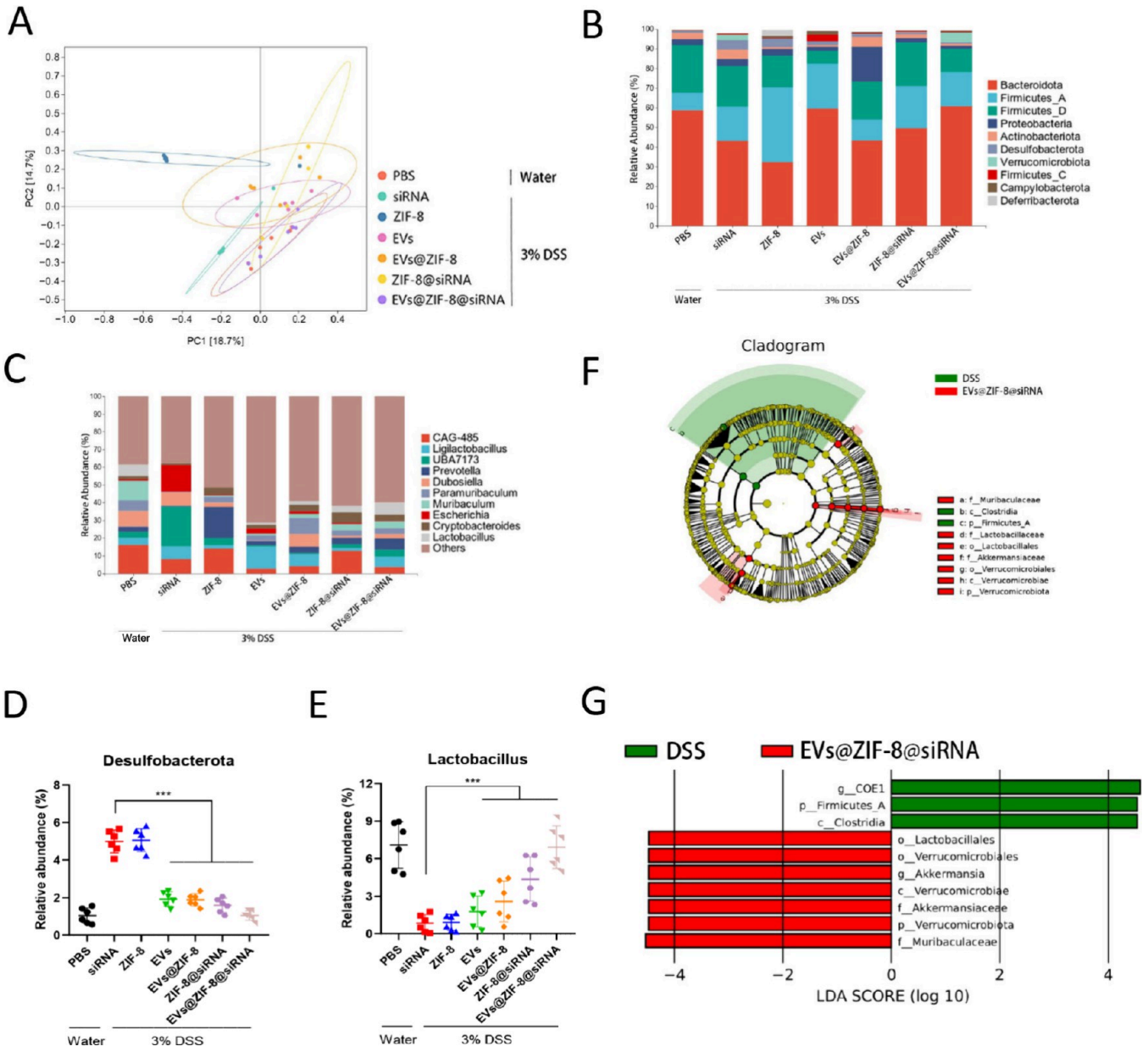

Figure 5. Regulation of gut microbiome by EVs@ZIF-8@siRNA in UC mice. (A) Principal coordinate analysis (PCoA) diagrams illustrating the diversity of microbiota (n = 6). (B) Column diagram of the relative abundance of the gut microbiome at phyla and (C) genus levels (n = 6). (D) Relative abundance of the representative bacterial groups at phyla and (E) genus levels (n = 6). (F) Cladogram based on linear discriminant analysis effect size (LEfSe) showing the difference of gut microbiota between the DSS group and EVs@ZIF-8@siRNA group (n = 6). (G) Phylogenetic distribution histogram based on the LDA score. Data are presented as the means ± SD. ***P < 0.001.

tissues were collected and analyzed. Compared with healthy mice, DSS mice treated with free siRNA and ZIF-8 were significantly shorted, while a remarkable recovery was achieved after treatment with EVs@ZIF-8@siRNA (Figure 4G, H). A slight increase in colon length was also observed in groups of EVs, EVs@ZIF-8 and ZIF-8@siRNA. These results confirmed that EVs@ZIF-8@siRNA nanoparticles can effectively deliver siRNA to colon tissue with targeting and enhance the UC therapeutic efficiency, owing to the combination of ginger-derived EVs and TNF-α siRNA payload.

Next, we examined the concentrations of proinflammatory cytokines (TNF-α, IL-6, and IL-1β) in the supernatants of colon tissue homogenates (Figure 4I–K). As shown in Figure 4I, a high expression of TNF-α in colon tissue was observed in free siRNA and ZIF-8 treated groups. However, the level of TNF-α was decreased after treatment with EVs, ZIF-8@siRNA and EVs@ZIF-8@siRNA, and EVs@ZIF-8@siRNA decreased the most. The results suggested that siRNA loaded in ZIF-8 can cooperate with ginger EVs to reduce the level of TNF-α. These proinflammatory cytokine levels of IL-6 and IL-1β were also tested. Figure 4J and K showed that their expressions were decreased to similar degrees after treatment with EVs, EVs@ZIF-8, and EVs@ZIF-8@siRNA. The reason for these results was that ginger EVs contained 6-shogaol, which had anti-inflammatory effects. So, these results further confirmed that EVs@ZIF-8 nanoparticles can deliver siRNA to colon tissue effectively to reduce the level of TNF-α and can work

https://doi.org/10.1021/acsami.4c10562
ACS Appl. Mater. Interfaces XXXX, XXX, XXX−XXX

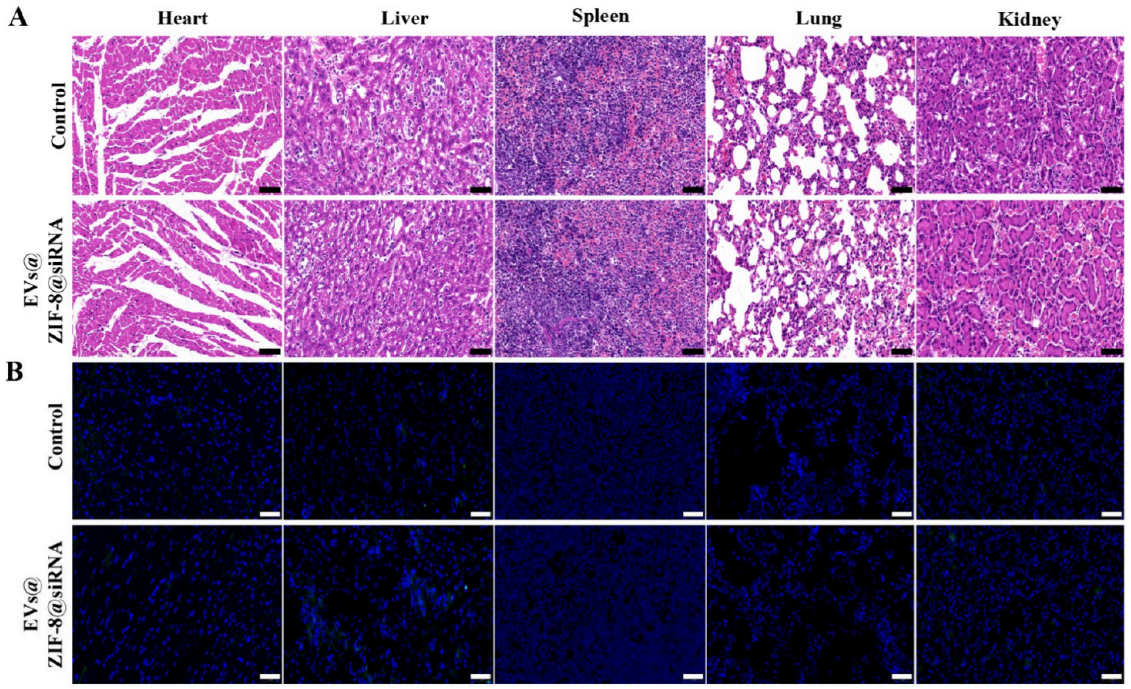

Figure 6. Biosafety of EVs@ZIF-8@siRNA *in vivo*. (A) Representative H&E and (B) fluorescent TUNEL staining of major organs. Scale bar = 50 μm.

synergistically with ginger EVs to reduced the levels of inflammatory factors.

Additionally, the activity of myeloperoxidase (MPO) was examined in colon tissue. MPO is a major inflammatory mediator in the pathogenesis of UC and a direct indicator of neutrophil infiltration in colon mucosa.[58] The results of MPO levels in colon tissue were reduced after treatment with EVs, EVs@ZIF-8, ZIF-8@siRNA and EVs@ZIF-8@siRNA, and the level in the EVs@ZIF-8@siRNA group was much lower than those for the other groups (Figure 4L). To evaluate the gene silencing efficiency of the siRNA payload by nanoparticles, the mRNA levels of TNF-α in the colon tissue were determined by qRT-PCR (Figure 4M−O), and these results were consistent with the inflammatory cytokine levels, indicating that EVs@ZIF-8@siRNA can inhibit the expression of TNF-α via the combination effects of ginger EVs and the TNF-α siRNA payload. Moreover, histological analysis also exhibited that the colon tissues of DSS mice showed the best intestinal epithelial repair after treatment with EVs@ZIF-8@siRNA (Figure 4P). Overall, these results suggested that EVs@ZIF-8@siRNA possessed a synergistic therapeutic effect against DSS-induced UC by combining the silencing effect of siRNA with the anti-inflammatory effect of ginger EVs.

3.5. Regulation of Gut Microbiome by EVs@ZIF-8@siRNA. Increasing evidence has shown that homeostasis of gut microbes is closely related to UC.[59−62] Therefore, 16S rRNA amplicon sequencing was performed using mouse fecal samples to explore whether EVs@ZIF-8@siRNA nanoparticles could regulate the gut microbiome composition and influence UC progression. Principal component analysis (PCoA) showed that samples in the EVs@ZIF-8@siRNA treated group formed a cluster distinct from the siRNA and ZIF-8 groups and more closely resembled healthy mice, suggesting that EVs@ZIF-8@siRNA could restore gut microbiome homeostasis to the healthy status. The ZIF-8@siRNA treated group was also distinguished from the siRNA and ZIF-8 groups, which indicated that ZIF-8@siRNA had limited microbial repair ability. However, EVs and EVs@ZIF-8 were less effective in regulating intestinal microbial, as their clusters were overlapped with the siRNA and ZIF-8 groups (Figure 5A). Cluster analysis at the phylum level was also performed, and results showed that compared to healthy mice, the abundance of *Bacteroidota* (an important bacterial phylum in the intestinal ecosystem involved in a variety of metabolism in the colon) was decreased in the siRNA and ZIF-8 groups and increased after EVs, EVs@ZIF-8, ZIF-8@siRNA and EVs@ZIF-8@siRNA treatment (Figure 5B). Moreover, groups treated with EVs, EVs@ZIF-8, ZIF-8@siRNA, and EVs@ZIF-8@siRNA displayed a remarkable reduction in the abundance of *Desulfobacterota* (known to play a harmful role in animal models of UC) in comparison with the siRNA and ZIF-8 groups, and the EVs@ZIF-8@siRNA group was closer to normal mice (Figure 5B, D). This result suggested that EVs@ZIF-8@siRNA could exert a therapeutic efficacy by regulating the relative abundance and composition of gut microbiota.[63−65] The gut microbiome structure was further analyzed at the genus level. Mice treated with EVs@ZIF-8@siRNA increased the abundance of beneficial gut bacteria, such as *Lactobacillus* (Figure 5C, E), which can strengthen gut barrier integrity and promote gut health by colonizing the intestine.[66,67] The difference of the microbial community between the DSS group and the EVs@ZIF-8@siRNA group was also analyzed by LEfSe. Results revealed that the species and abundance of gut microbiome were decreased in DSS group mice, while they increased in the EVs@ZIF-8@siRNA group with enriched probiotics like *Lactobacillales* and *Akkermansia* (enriched in human and animal gut, which can improve intestinal barrier function) (Figure 5F, G).[68−70] Overall, these findings suggested that EVs@ZIF-8@siRNA can effectively regulate the gut microbiome composition and abundance in UC mice, thereby facilitating intestinal epithelial repair to contribute to the UC treatment.

https://doi.org/10.1021/acsami.4c10562
ACS Appl. Mater. Interfaces XXXX, XXX, XXX−XXX

3.6. Biosafety of EVs@ZIF-8@siRNA. The biosafety of EVs@ZIF-8@siRNA on major organs was also evaluated using histological analysis. According to the H&E-stained section results, the overall structure and integrity of heart, liver, spleen, lung and kidney tissues in mice showed no significant difference between the EVs@ZIF-8@siRNA treated group and normal mice (Figure 6A). Fluorescent TUNEL staining images also showed that apoptosis levels in major tissues treated with EVs@ZIF-8@siRNA were similar to those of the healthy control (Figure 6B). These results suggested that EVs@ZIF-8@siRNA nanoparticles displayed good biosafety in the long-time treatment and showed potential for the UC therapy.

4. CONCLUSIONS

In summary, a novel ginger EVs-coated ZIF-8 nanodelivery system is designed and has been proven to deliver siRNA effectively for UC targeted therapy. ZIF-8 is used to efficiently encapsulate and deliver TNF-α-specific siRNA; ginger EVs coating enhances the acid resistance and facilitates colon tissue targeting. *In vitro* experiments have shown that ginger EVs greatly improved the uptake of EVs@ZIF-8@siRNA nanoparticles by macrophages, and siRNA in the nanoparticles can effectively inhibit the targeted TNF-α. Animal experiments have demonstrated that TNF-α siRNA loaded in the nanocarrier can work synergistically with 6-shogaol in ginger EVs to enhance the therapeutic effect, and show good colon targeting and safety. These positive results demonstrate that EVs@ZIF-8@siRNA nanoparticles are an efficient siRNA delivery system, which can increase the colon targeting and enhance the UC therapeutic efficacy by combing with ginger-derived EVs. Moreover, EVs@ZIF-8@siRNA treatment has been found to restore the composite and abundance of gut microbiota to healthy status, making this system suitable as an orally administrated reagent for UC therapy. Therefore, we believe that the system proposed in this study will provide a new perspective on UC personalized therapies.

■ ASSOCIATED CONTENT

Supporting Information

The Supporting Information is available free of charge at https://pubs.acs.org/doi/10.1021/acsami.4c10562.

DLS size changes of ginger EVs with time at pH 3.0; fluorescence overlap analysis of RAW 264.7 cells incubated with nanoparticles for different time; stability of EVs@ZIF-8@siRNA over time in PBS at different pH values; SDS-PAGE, DLS and TEM of ginger EVs stored at −80 °C for 48 h; effects of different nanoparticles on Caco-2 cell and HT-29 cell viability; HPLC trace data of EVs and EVs@ZIF-8@siRNA. (PDF)

■ AUTHOR INFORMATION

Corresponding Authors

Zhaowei Sun − *School of Life Sciences, Zhengzhou University, Zhengzhou 450001 Henan, China*; Email: szw@zzu.edu.cn

Haibo Weng − *School of Life Sciences, Zhengzhou University, Zhengzhou 450001 Henan, China*; orcid.org/0000-0002-9527-1289; Email: whb@zzu.edu.cn

Authors

Chenyang Cui − *School of Life Sciences, Zhengzhou University, Zhengzhou 450001 Henan, China*

Miao Du − *School of Life Sciences, Zhengzhou University, Zhengzhou 450001 Henan, China*

Yihang Zhao − *School of Life Sciences, Zhengzhou University, Zhengzhou 450001 Henan, China*

Jiaze Tang − *School of Life Sciences, Zhengzhou University, Zhengzhou 450001 Henan, China*

Mengge Liu − *School of Life Sciences, Zhengzhou University, Zhengzhou 450001 Henan, China*

Geng Min − *School of Life Sciences, Zhengzhou University, Zhengzhou 450001 Henan, China*

Rongchen Chen − *School of Life Sciences, Zhengzhou University, Zhengzhou 450001 Henan, China*

Qiang Zhang − *Department of Critical Care Medicine, The Fifth Affiliated Hospital of Zhengzhou University, Zhengzhou 450052 Henan, China*

Complete contact information is available at: https://pubs.acs.org/10.1021/acsami.4c10562

Author Contributions

Chenyang Cui: Conceptualization, Date curation, Formal analysis, Investigation, Methodology, Software, Writing−original draft. Miao Du: Investigation, Data curation, Formal analysis, Investigation, Methodology, Software. Yihang Zhao: Data curation, Investigation, Methodology, Supervision. Jiaze Tang: Data curation, Formal analysis, Investigation, Methodology. Mengge Liu: Software, Validation, Visualization. Geng Min: Formal analysis, Validation. Rongchen Chen: Methodology, Software. Qiang Zhang: Methodology, Software. Zhaowei Sun: Conceptualization, Funding acquisition, Project administration, Resources, Supervision, Validation, Writing−review and editing. Haibo Weng: Conceptualization, Funding acquisition, Project administration, Resources, Supervision, Validation, Visualization, Writing−review and editing.

Notes

The authors declare no competing financial interest.

Ethics Approval and Consent to Participate. All animal experiments were conducted under the Regional Ethics Committee for Animal Experiments at Zhengzhou University.

■ ACKNOWLEDGMENTS

This work was supported by the National Natural Science Foundation of China (No. 81970173, No. 82402437) and the China Postdoctoral Science Foundation (No. 2022M712875). The authors are grateful for the technical support provided by the Modern Analysis and Computer Center of Zhengzhou University. Graphical Abstract and Scheme 1 were created with biorender.com.

■ REFERENCES

(1) Kuenzig, M. E.; Fung, S. G.; Marderfeld, L.; Mak, J. W. Y.; Kaplan, G. G.; Ng, S. C.; Wilson, D. C.; Cameron, F.; Henderson, P.; Kotze, P. G.; et al. Twenty-first Century Trends in the Global Epidemiology of Pediatric-Onset Inflammatory Bowel Disease: Systematic Review. *Gastroenterology* **2022**, *162* (4), 1147−1159.

(2) D'Alessio, S.; Ungaro, F.; Noviello, D.; Lovisa, S.; Peyrin-Biroulet, L.; Danese, S. Revisiting fibrosis in inflammatory bowel disease: the gut thickens. *Nat. Rev. Gastroenterol Hepatol* **2022**, *19* (3), 169−184.

(3) Le Berre, C.; Honap, S.; Peyrin-Biroulet, L. Ulcerative colitis. *Lancet* **2023**, *402* (10401), 571−584.

(4) Zhou, Y.; Yang, M.; Yan, X.; Zhang, L.; Lu, N.; Ma, Y.; Zhang, Y.; Cui, M.; Zhang, M.; Zhang, M. Oral Nanotherapeutics of Andrographolide/Carbon Monoxide Donor for Synergistically Anti-

inflammatory and Pro-resolving Treatment of Ulcerative Colitis. *ACS Appl. Mater. Interfaces* **2023**, *15* (30), 36061−36075.
(5) Fairbrass, K. M.; Costantino, S. J.; Gracie, D. J.; Ford, A. C. Prevalence of irritable bowel syndrome-type symptoms in patients with inflammatory bowel disease in remission: a systematic review and meta-analysis. *Lancet Gastroenterol Hepatol* **2020**, *5* (12), 1053−1062.
(6) Yan, X.; Meng, L.; Zhang, X.; Deng, Z.; Gao, B.; Zhang, Y.; Yang, M.; Ma, Y.; Zhang, Y.; Tu, K.; et al. Reactive oxygen species-responsive nanocarrier ameliorates murine colitis by intervening colonic innate and adaptive immune responses. *Mol. Ther* **2023**, *31* (5), 1383−1401.
(7) Vermeire, S. Combination biologic therapy for ulcerative colitis. *Lancet Gastroenterol Hepatol* **2023**, *8* (4), 288−290.
(8) Okumura, R.; Takeda, K. Maintenance of intestinal homeostasis by mucosal barriers. *Inflamm Regen* **2018**, *38*, 5.
(9) Chen, Y.; Mai, Q.; Chen, Z.; Lin, T.; Cai, Y.; Han, J.; Wang, Y.; Zhang, M.; Tan, S.; Wu, Z.; et al. Dietary palmitoleic acid reprograms gut microbiota and improves biological therapy against colitis. *Gut Microbes* **2023**, *15* (1), 2211501.
(10) Lee, J.; Son, W.; Hong, J.; Song, Y.; Yang, C. S.; Kim, Y. H. Down-regulation of TNF-α via macrophage-targeted RNAi system for the treatment of acute inflammatory sepsis. *J. Controlled Release* **2021**, *336*, 344−353.
(11) Li, D.; Shangguan, J.; Yu, F.; Lin, G.; Pan, H.; Zhang, M.; Lin, H.; Chen, B.; Xu, H.; Hu, S. Growth Factors-Loaded Temperature-Sensitive Hydrogel as Biomimetic Mucus Attenuated Murine Ulcerative Colitis via Repairing the Mucosal Barriers. *ACS Appl. Mater. Interfaces* **2024**, *16* (6), 7686−7699.
(12) Atreya, R.; Zimmer, M.; Bartsch, B.; Waldner, M. J.; Atreya, I.; Neumann, H.; Hildner, K.; Hoffman, A.; Kiesslich, R.; Rink, A. D.; et al. Antibodies against tumor necrosis factor (TNF) induce T-cell apoptosis in patients with inflammatory bowel diseases via TNF receptor 2 and intestinal CD14$^+$ macrophages. *Gastroenterology* **2011**, *141* (6), 2026−2038.
(13) Kayal, M.; Shah, S. Ulcerative Colitis: Current and Emerging Treatment Strategies. *J. Clin Med.* **2020**, *9* (1), 94.
(14) Hirten, R. P.; Sands, B. E. New Therapeutics for Ulcerative Colitis. *Annu. Rev. Med.* **2021**, *72*, 199−213.
(15) Wang, J.; Chen, G.; Liu, N.; Han, X.; Zhao, F.; Zhang, L.; Chen, P. Strategies for improving the safety and RNAi efficacy of noncovalent peptide/siRNA nanocomplexes. *Adv. Colloid Interface Sci.* **2022**, *302*, 102638.
(16) Dong, Y.; Siegwart, D. J.; Anderson, D. G. Strategies, design, and chemistry in siRNA delivery systems. *Adv. Drug Deliv Rev.* **2019**, *144*, 133−147.
(17) Parodi, A.; Buzaeva, P.; Nigovora, D.; Baldin, A.; Kostyushev, D.; Chulanov, V.; Savvateeva, L. V.; Zamyatnin, A. A., Jr Nanomedicine for increasing the oral bioavailability of cancer treatments. *J. Nanobiotechnology* **2021**, *19* (1), 354.
(18) Deng, J.; Zhu, X.; Chen, Z.; Fan, C. H.; Kwan, H. S.; Wong, C. H.; Shek, K. Y.; Zuo, Z.; Lam, T. N. A Review of Food-Drug Interactions on Oral Drug Absorption. *Drugs* **2017**, *77* (17), 1833−1855.
(19) Zhou, X.; Yu, M.; Ma, L.; Fu, J.; Guo, J.; Lei, J.; Fu, Z.; Fu, Y.; Zhang, Q.; Zhang, C. Y.; et al. In vivo self-assembled siRNA as a modality for combination therapy of ulcerative colitis. *Nat. Commun.* **2022**, *13* (1), 5700.
(20) McCarthy, J.; O'Neill, M. J.; Bourre, L.; Walsh, D.; Quinlan, A.; Hurley, G.; Ogier, J.; Shanahan, F.; Melgar, S.; Darcy, R.; et al. Gene silencing of TNF-alpha in a murine model of acute colitis using a modified cyclodextrin delivery system. *J. Controlled Release* **2013**, *168* (1), 28−34.
(21) Frede, A.; Neuhaus, B.; Klopfleisch, R.; Walker, C.; Buer, J.; Müller, W.; Epple, M.; Westendorf, A. M. Colonic gene silencing using siRNA-loaded calcium phosphate/PLGA nanoparticles ameliorates intestinal inflammation in vivo. *J. Controlled Release* **2016**, *222*, 86−96.
(22) Kriegel, C.; Attarwala, H.; Amiji, M. Multi-compartmental oral delivery systems for nucleic acid therapy in the gastrointestinal tract. *Adv. Drug Deliv Rev.* **2013**, *65* (6), 891−901.
(23) Fan, Y.; Dhaliwal, H. K.; Menon, A. V.; Chang, J.; Choi, J. E.; Amiji, M. M.; Kim, J. Site-specific intestinal DMT1 silencing to mitigate iron absorption using pH-sensitive multi-compartmental nanoparticulate oral delivery system. *Nanomedicine* **2019**, *22*, 102091.
(24) Liu, S.; Wu, X.; Chandra, S.; Lyon, C.; Ning, B.; Jiang, L.; Fan, J.; Hu, T. Y. Extracellular vesicles: Emerging tools as therapeutic agent carriers. *Acta Pharm. Sin B* **2022**, *12* (10), 3822−3842.
(25) Cheng, L.; Hill, A. F. Therapeutically harnessing extracellular vesicles. *Nat. Rev. Drug Discov* **2022**, *21* (5), 379−399.
(26) Vader, P.; Mol, E. A.; Pasterkamp, G.; Schiffelers, R. M. Extracellular vesicles for drug delivery. *Adv. Drug Deliv Rev.* **2016**, *106* (Pt A), 148−156.
(27) Liu, X.; Cao, Z.; Wang, W.; Zou, C.; Wang, Y.; Pan, L.; Jia, B.; Zhang, K.; Zhang, W.; Li, W.; et al. Engineered Extracellular Vesicle-Delivered CRISPR/Cas9 for Radiotherapy Sensitization of Glioblastoma. *ACS Nano* **2023**, *17* (17), 16432−16447.
(28) Sung, J.; Alghoul, Z.; Long, D.; Yang, C.; Merlin, D. Oral delivery of IL-22 mRNA-loaded lipid nanoparticles targeting the injured intestinal mucosa: A novel therapeutic solution to treat ulcerative colitis. *Biomaterials* **2022**, *288*, 121707.
(29) Al-Suhaimi, E. A.; Al-Riziza, N. A.; Al-Essa, R. A. Physiological and therapeutical roles of ginger and turmeric on endocrine functions. *Am. J. Chin Med.* **2011**, *39* (2), 215−231.
(30) Liu, C.; Yan, X.; Zhang, Y.; Yang, M.; Ma, Y.; Zhang, Y.; Xu, Q.; Tu, K.; Zhang, M. Oral administration of turmeric-derived exosome-like nanovesicles with anti-inflammatory and pro-resolving bioactions for murine colitis therapy. *J. Nanobiotechnology* **2022**, *20* (1), 206.
(31) Ju, S.; Mu, J.; Dokland, T.; Zhuang, X.; Wang, Q.; Jiang, H.; Xiang, X.; Deng, Z. B.; Wang, B.; Zhang, L.; et al. Grape exosome-like nanoparticles induce intestinal stem cells and protect mice from DSS-induced colitis. *Mol. Ther* **2013**, *21* (7), 1345−1357.
(32) Yang, F.; Dong, J.; Li, Z.; Wang, Z. Metal-Organic Frameworks (MOF)-Assisted Sonodynamic Therapy in Anticancer Applications. *ACS Nano* **2023**, *17* (5), 4102−4133.
(33) Khezri, B.; Pumera, M. Metal-Organic Frameworks Based Nano/Micro/Millimeter-Sized Self-Propelled Autonomous Machines. *Adv. Mater.* **2019**, *31* (14), No. e1806530.
(34) Ma, Y.; Gao, W.; Zhang, Y.; Yang, M.; Yan, X.; Zhang, Y.; Li, G.; Liu, C.; Xu, C.; Zhang, M. Biomimetic MOF Nanoparticles Delivery of C-Dot Nanozyme and CRISPR/Cas9 System for Site-Specific Treatment of Ulcerative Colitis. *ACS Appl. Mater. Interfaces* **2022**, *14* (5), 6358−6369.
(35) Zhang, M.; Viennois, E.; Prasad, M.; Zhang, Y.; Wang, L.; Zhang, Z.; Han, M. K.; Xiao, B.; Xu, C.; Srinivasan, S.; et al. Edible ginger-derived nanoparticles: A novel therapeutic approach for the prevention and treatment of inflammatory bowel disease and colitis-associated cancer. *Biomaterials* **2016**, *101*, 321−340.
(36) Zhang, M.; Xu, C.; Liu, D.; Han, M. K.; Wang, L.; Merlin, D. Oral Delivery of Nanoparticles Loaded With Ginger Active Compound, 6-Shogaol, Attenuates Ulcerative Colitis and Promotes Wound Healing in a Murine Model of Ulcerative Colitis. *J. Crohns Colitis* **2018**, *12* (2), 217−229.
(37) Cui, C.; He, Q.; Wang, J.; Kang, J.; Ma, W.; Nian, Y.; Sun, Z.; Weng, H. Targeted miR-34a delivery with PD1 displayed bacterial outer membrane vesicles-coated zeolitic imidazolate framework nanoparticles for enhanced tumor therapy. *Int. J. Biol. Macromol.* **2023**, *247*, 125692.
(38) Qiao, Z.; Zhang, K.; Liu, J.; Cheng, D.; Yu, B.; Zhao, N.; Xu, F. J. Biomimetic electrodynamic nanoparticles comprising ginger-derived extracellular vesicles for synergistic anti-infective therapy. *Nat. Commun.* **2022**, *13* (1), 7164.
(39) O'Mahony, A. M.; Ogier, J.; Desgranges, S.; Cryan, J. F.; Darcy, R.; O'Driscoll, C. M. A click chemistry route to 2-functionalised PEGylated and cationic β-cyclodextrins: co-formulation opportunities for siRNA delivery. *Org. Biomol Chem.* **2012**, *10* (25), 4954−4960.

https://doi.org/10.1021/acsami.4c10562
ACS Appl. Mater. Interfaces XXXX, XXX, XXX−XXX

(40) Zhao, C.; Yang, J.; Chen, M.; Chen, W.; Yang, X.; Ye, H.; Wang, L.; Wang, Y.; Shi, J.; Yue, F.; et al. Synthetic Lignin-Derived Therapeutic Nano Reagent as Intestinal pH-Sensitive Drug Carriers Capable of Bypassing the Gastric Acid Environment for Colitis Treatment. *ACS Nano* **2023**, *17* (1), 811−824.
(41) Guo, Y.; He, X.; Zhao, R. M.; Yang, H. Z.; Huang, Z.; Zhang, J.; Yu, X. Q. Zn-dipicolylamine-based reactive oxygen species-responsive lipids for siRNA delivery and in vivo colitis treatment. *Acta Biomater* **2022**, *147*, 287−298.
(42) Gao, M.; Yang, C.; Wu, C.; Chen, Y.; Zhuang, H.; Wang, J.; Cao, Z. Hydrogel-metal-organic-framework hybrids mediated efficient oral delivery of siRNA for the treatment of ulcerative colitis. *J. Nanobiotechnology* **2022**, *20* (1), 404.
(43) Teng, Y.; Ren, Y.; Sayed, M.; Hu, X.; Lei, C.; Kumar, A.; Hutchins, E.; Mu, J.; Deng, Z.; Luo, C.; et al. Plant-Derived Exosomal MicroRNAs Shape the Gut Microbiota. *Cell Host Microbe* **2018**, *24* (5), 637−652.
(44) Wang, Z.; Fu, Y.; Kang, Z.; Liu, X.; Chen, N.; Wang, Q.; Tu, Y.; Wang, L.; Song, S.; Ling, D.; et al. Organelle-Specific Triggered Release of Immunostimulatory Oligonucleotides from Intrinsically Coordinated DNA-Metal-Organic Frameworks with Soluble Exoskeleton. *J. Am. Chem. Soc.* **2017**, *139* (44), 15784−15791.
(45) Luk, B. T.; Hu, C. M.; Fang, R. H.; Dehaini, D.; Carpenter, C.; Gao, W.; Zhang, L. Interfacial interactions between natural RBC membranes and synthetic polymeric nanoparticles. *Nanoscale* **2014**, *6* (5), 2730−2737.
(46) Zhuang, J.; Duan, Y.; Zhang, Q.; Gao, W.; Li, S.; Fang, R. H.; Zhang, L. Multimodal Enzyme Delivery and Therapy Enabled by Cell Membrane-Coated Metal-Organic Framework Nanoparticles. *Nano Lett.* **2020**, *20* (5), 4051−4058.
(47) Gao, J.; Chu, W.; Ding, X.; Ding, L.; Guo, Q.; Fu, Y. Degradation Kinetic Studies of BSA@ZIF-8 Nanoparticles with Various Zinc Precursors, Metal-to-Ligand Ratios, and pH Conditions. *ACS Omega* **2023**, *8* (47), 44601−44610.
(48) Zhuang, J.; Kuo, C. H.; Chou, L. Y.; Liu, D. Y.; Weerapana, E.; Tsung, C. K. Optimized metal-organic-framework nanospheres for drug delivery: evaluation of small-molecule encapsulation. *ACS Nano* **2014**, *8* (3), 2812−2819.
(49) Yong, T.; Wei, Z.; Gan, L.; Yang, X. Extracellular-Vesicle-Based Drug Delivery Systems for Enhanced Antitumor Therapies through Modulating the Cancer-Immunity Cycle. *Adv. Mater.* **2022**, *34* (52), No. e2201054.
(50) Kim, M.; Lee, J. S.; Kim, W.; Lee, J. H.; Jun, B. H.; Kim, K. S.; Kim, D. E. Aptamer-conjugated nano-liposome for immunogenic chemotherapy with reversal of immunosuppression. *J. Controlled Release* **2022**, *348*, 893−910.
(51) Björnmalm, M.; Thurecht, K. J.; Michael, M.; Scott, A. M.; Caruso, F. Bridging Bio-Nano Science and Cancer Nanomedicine. *ACS Nano* **2017**, *11* (10), 9594−9613.
(52) Ochando, J.; Mulder, W. J. M.; Madsen, J. C.; Netea, M. G.; Duivenvoorden, R. Trained immunity - basic concepts and contributions to immunopathology. *Nat. Rev. Nephrol* **2023**, *19* (1), 23−37.
(53) He, W.; Kapate, N.; Shields, C. W. t.; Mitragotri, S. Drug delivery to macrophages: A review of targeting drugs and drug carriers to macrophages for inflammatory diseases. *Adv. Drug Deliv Rev.* **2020**, *165*−*166*, 15−40.
(54) Hu, C. M.; Zhang, L.; Aryal, S.; Cheung, C.; Fang, R. H.; Zhang, L. Erythrocyte membrane-camouflaged polymeric nanoparticles as a biomimetic delivery platform. *Proc. Natl. Acad. Sci. U. S. A.* **2011**, *108* (27), 10980−10985.
(55) Chen, Q.; Bai, H.; Wu, W.; Huang, G.; Li, Y.; Wu, M.; Tang, G.; Ping, Y. Bioengineering Bacterial Vesicle-Coated Polymeric Nanomedicine for Enhanced Cancer Immunotherapy and Metastasis Prevention. *Nano Lett.* **2020**, *20* (1), 11−21.
(56) Wu, Z.; Huang, S.; Li, T.; Li, N.; Han, D.; Zhang, B.; Xu, Z. Z.; Zhang, S.; Pang, J.; Wang, S.; et al. Gut microbiota from green tea polyphenol-dosed mice improves intestinal epithelial homeostasis and ameliorates experimental colitis. *Microbiome* **2021**, *9* (1), 184.
(57) Guo, H.; Guo, H.; Xie, Y.; Chen, Y.; Lu, C.; Yang, Z.; Zhu, Y.; Ouyang, Y.; Zhang, Y.; Wang, X. Mo(3)Se(4) nanoparticle with ROS scavenging and multi-enzyme activity for the treatment of DSS-induced colitis in mice. *Redox Biol.* **2022**, *56*, 102441.
(58) He, H.; Zheng, N.; Song, Z.; Kim, K. H.; Yao, C.; Zhang, R.; Zhang, C.; Huang, Y.; Uckun, F. M.; Cheng, J.; et al. Suppression of Hepatic Inflammation via Systemic siRNA Delivery by Membrane-Disruptive and Endosomolytic Helical Polypeptide Hybrid Nanoparticles. *ACS Nano* **2016**, *10* (2), 1859−1870.
(59) Baumgartner, M.; Zirnbauer, R.; Schlager, S.; Mertens, D.; Gasche, N.; Sladek, B.; Herbold, C.; Bochkareva, O.; Emelianenko, V.; Vogelsang, H.; et al. Atypical enteropathogenic E. coli are associated with disease activity in ulcerative colitis. *Gut Microbes* **2022**, *14* (1), 2143218.
(60) Lang, S.; Schnabl, B. Microbiota and Fatty Liver Disease-the Known, the Unknown, and the Future. *Cell Host Microbe* **2020**, *28* (2), 233−244.
(61) Zhang, Z.; Pan, Y.; Guo, Z.; Fan, X.; Pan, Q.; Gao, W.; Luo, K.; Pu, Y.; He, B. An olsalazine nanoneedle-embedded inulin hydrogel reshapes intestinal homeostasis in inflammatory bowel disease. *Bioact Mater.* **2024**, *33*, 71−84.
(62) Fan, X.; Zhang, Z.; Gao, W.; Pan, Q.; Luo, K.; He, B.; Pu, Y. An Engineered Butyrate-Derived Polymer Nanoplatform as a Mucosa-Healing Enhancer Potentiates the Therapeutic Effect of Magnolol in Inflammatory Bowel Disease. *ACS Nano* **2024**, *18* (1), 229−244.
(63) Xie, R.; Gu, Y.; Li, M.; Li, L.; Yang, Y.; Sun, Y.; Zhou, B.; Liu, T.; Wang, S.; Liu, W.; et al. Desulfovibrio vulgaris interacts with novel gut epithelial immune receptor LRRC19 and exacerbates colitis. *Microbiome* **2024**, *12* (1), 4.
(64) Zhao, X.; Jiang, L.; Fang, X.; Guo, Z.; Wang, X.; Shi, B.; Meng, Q. Host-microbiota interaction-mediated resistance to inflammatory bowel disease in pigs. *Microbiome* **2022**, *10* (1), 115.
(65) Ley, R. E.; Turnbaugh, P. J.; Klein, S.; Gordon, J. I. Microbial ecology: human gut microbes associated with obesity. *Nature* **2006**, *444* (7122), 1022−1023.
(66) Barnett, A. M.; Roy, N. C.; Cookson, A. L.; McNabb, W. C. Metabolism of Caprine Milk Carbohydrates by Probiotic Bacteria and Caco-2:HT29$^-$MTX Epithelial Co-Cultures and Their Impact on Intestinal Barrier Integrity. *Nutrients* **2018**, *10* (7), 949.
(67) Anderson, R. C.; Cookson, A. L.; McNabb, W. C.; Park, Z.; McCann, M. J.; Kelly, W. J.; Roy, N. C. Lactobacillus plantarum MB452 enhances the function of the intestinal barrier by increasing the expression levels of genes involved in tight junction formation. *BMC Microbiol* **2010**, *10*, 316.
(68) Zhai, Q.; Feng, S.; Arjan, N.; Chen, W. A next generation probiotic, Akkermansia muciniphila. *Crit Rev. Food Sci. Nutr* **2019**, *59* (19), 3227−3236.
(69) Cani, P. D.; Depommier, C.; Derrien, M.; Everard, A.; de Vos, W. M. Author Correction: Akkermansia muciniphila: paradigm for next-generation beneficial microorganisms. *Nat. Rev. Gastroenterol Hepatol* **2022**, *19* (10), 682.
(70) Ma, D. X.; Zhou, Y.; Wu, L. D.; Li, Z. Y.; Jiang, W. J.; Huang, S. L.; Guo, X. P.; Sheng, J. Z.; Wang, F. S. Enhanced Stability and Function of Probiotic Streptococcus thermophilus with Self-Encapsulation by Increasing the Biosynthesis of Hyaluronan. *ACS Appl. Mater. Interfaces* **2022**, *14* (38), 42963−42975.

https://doi.org/10.1021/acsami.4c10562
ACS Appl. Mater. Interfaces XXXX, XXX, XXX−XXX